

Copper nanowire array as highly selective electrochemical sensor of nitrate ions in water

B. Patella^a, R. R. Russo^a, A. O'Riordan^b, G. Aiello^a, C. Sunseri^a and R. Inguanta^{a1}

^aLaboratorio di Chimica Fisica Applicata, Dipartimento di Ingegneria
Università of Palermo, Viale delle Scienze, Palermo, Italy

^bNanotechnology group, Tyndall National Institute
University College Cork, Dyke Parade, Cork, Ireland

Abstract

Contamination of water with nitrate ions is a significant problem that affects many areas of the world. The danger from nitrates is not so much their toxicity, rather low, as their transformation into nitrites and in particular into nitrosamines, substances considered to be a possible carcinogenic risk. For this reason, European legislation has set the maximum permissible concentration of nitrates in drinking water at 44 mg/l. Thus, it is clear that a continuous monitoring of nitrate ions is of high technological interest but it must be rapid, easy to perform and directly performable in situ. Electrochemical detection is certainly among the best techniques to obtain the above requirements. In particular, in this work we have developed a nanostructured sensor based on array of copper nanowires obtained with the simple method of galvanic deposition. The nanostructured sensors have a very short response time with a detection limit less than 10 μ M. Different interfering species were tested finding a negligible effect except for the chlorine ions. However, this problem has been solved by removing chlorine ions from the water through a simple precipitation of chloride compounds with low solubility. Nanostructured sensors were also used to analyze real water samples (rain, river and drinking water). In the case of drinking water, we have measured a concentration of nitrate ions very close to the that measured by conventional laboratory techniques.

¹ Corresponding author: R. Inguanta, rosalinda.inguanta@unipa.it

26 **Keywords:** Electrochemical sensor; Copper; Nitrate ion; Water contamination; Galvanic
27 deposition; Nanowire.

28 **1. Introduction**

29 In the last decades, the contamination of water with nitrate ions is of more and more
30 importance. Agricultural and livestock sectors are the main sources of nitrate contamination [1]. In
31 fact, nitrogen-based fertilizers are highly used in agriculture and their over-use leads to a release of
32 nitrate ions directly in ground water with the consequent contamination of the food chain. High
33 nitrate concentration in the aquatic environment leads to the overgrowth of algae causing an oxygen
34 depletion (eutrophication) that is highly harmful for aquatic species [2]. High level of nitrate ions, is
35 also dangerous for human health [3][4], because they are converted into different harmful nitrogen
36 based compound such as nitrite, nitric oxide, N-nitroso compounds [5,6] that are responsible of
37 several diseases: such as cancer, Parkinson and gastritis [7–9]. More important, nitrate ions are
38 responsible of the blue-baby syndrome (or methemoglobinemia), due to the oxidation of the
39 hemoglobin in methemoglobin by nitrate ions that have a lower capability to oxygen transport
40 [10,11].

41 For these reasons, the Acceptable Daily Intake (ADI) of nitrate has been imposed at 3.7
42 mg/kg body-weight by the Food and Agriculture Organization (FAO) of the United Nation (UN)
43 and by the World Health Organization (WHO) in 2002 [4], [7]. Besides, the Environmental
44 Protection Agency (EPA), has established the maximum amount of nitrates ions in drinkable water
45 at 44 mg/L, limit that is also valid in many European countries [12]. Therefore, it is clear that
46 monitoring the ecological concentration of nitrates has gained increasing importance. Many
47 techniques can be used to detect nitrates but generally the choice depends on the sample nature, the
48 expected nitrate concentration and the kind of required analysis (time, in situ). Generally,
49 spectroscopy techniques are the most used because allow to carry out analyses with high precision
50 and reaching low LOD [13]. However, these techniques require skilled workforces and specific

51 instrumentations, besides the procedure is long and hard (i.e. the conversion of nitrates in nitrites by
52 using cadmium or zinc salts, preparation of standards) [14], [2].

53 In this context, is clear that the development of an easy, fast and not-lab-depended
54 technology to detect nitrate ions is of great importance and can help the continuously monitoring
55 the pollution of natural water. Electrochemical sensors are perfect candidates to overcome all these
56 limits, being fast, cheap, easy to use and can work with simple and small instrumentations [15–20].
57 Different type of electrochemical sensors have been exploited in order to quantify nitrates, such as
58 impedimetric [21]; [22], chronoamperometric [23–27], voltammetric [28]; [29–33] and also
59 biosensors [34,35], [36]. As concern the enzymatic biosensors they permit to obtain very low Limit
60 Of Detection (LOD) but the detection is very hard, expensive and time consuming (accurate pH
61 control, many separation and incubation steps) [37]. Many different electrode materials have been
62 tested and studied for nitrate ions detection but, in the last years, researchers have focused on
63 copper based electrodes due to its low overpotential for reduction of nitrate ions [38]. Davis et al.
64 [39] developed a macro-porous copper electrode founding a LOD of about 10 mM. In recent years,
65 this LOD has been decreased by using nanosized copper electrodes. For example, Essoussi et al. [40]
66 using a ion imprinted polymer coated with copper NPs have obtained a LOD of about 1000 times
67 lower that is probably due to the high surface area of nanoparticles. Similarly, others authors
68 [41,42] took advantage of the high surface area of copper NPs and the good electrical properties of
69 carbonaceous materials, such as carbon nanotubes and disposable pencil graphite, to detect nitrate
70 in a wide linear range. Interesting is also the approach followed by Wu et al [43] that have prepared
71 Cu nanowire array by electrochemical reduction of copper oxide nanowires obtained by thermal
72 oxidation. Using this electrode and the amperometric detection, have detected nitrate ions in the
73 linear range of 50 μM to 600 μM with a LOD of 12.2 μM .

74 In this work we have focused our attention on the possibility to use vertically standing
75 copper nanowires (Cu NWs) obtained by template galvanic deposition (GD) into nanoporous

76 membrane [44], [45]. The overall process is cost effective, scalable, fast and Cu NWs that are well
77 anchored to a copper current collector can be easily obtained. Furthermore, GD process can be used
78 to synthesize different kind of electrode materials, such as nickel [46,47]; [48], palladium [49,50],
79 amorphous silicon [51], compound of lead [52] and so on. Using this kind of nanostructured
80 electrode, the surface area of the sensor is about 70 time higher than bare ones and this is a special
81 property for electrochemical devices that should enhance their performance [18], [53], [16], [54].
82 Cu nanowires obtained by template electrodeposition were tested by Stortini et al [55] who found
83 very interesting results and obtained a very low LOD. They also demonstrated that the electrode is
84 able to detect nitrate ions in water sample containing interfering chloride ions at low concentration.

85 Considering the increase of activity of nanostructured copper, in this work we have studied
86 the performance of vertically standing Cu NWs obtained by the simple and low-cost method of GD
87 for nitrate detection in water by using Linear Sweep Voltammetry (LSV). A low LOD of about 9.1
88 μM , almost 100 times lower than the limit established by EPA and WHO that is about 750 μM (50
89 ppm), in a wide linear range was found. The effect of many interferences (chlorine, potassium,
90 sodium, sulfate, magnesium, carbonate anions, copper, lead, zinc, aluminum, mercury, nickel) will
91 be also shown and described. Finally, nitrate ions were also successfully detected in real samples
92 (river, rain and drinking water) demonstrating the real applicability of the proposed system.

93 **2. Experimental**

94 Commercial polycarbonate membranes (PoreticsTM) were used as template for copper GD.
95 The membrane has a thickness of about 8 μm and consists of interconnected cylindrical pore
96 (Figure S1) with a nominal mean diameter of about 200. Nanowires growth were performed
97 according to previous work [44]. Briefly, one surface of the membrane was sputtered with gold (for
98 1 minute) in order to make it conductive for the subsequent deposition of copper current collector
99 (about 12 μm thick). This step was carried out at constant current (8 mA/cm^2) for 1 h, in an
100 electrochemical cell containing a Pt mesh as a counter electrode and an aqueous solution of 0.2 M

101 $\text{CuSO}_4 \cdot 5\text{H}_2\text{O}$ and 0.1 M H_3BO_3 and powered by a PARSTAT galvanostat (mod. 2273). To obtain
102 Cu nanowire by GD, the current collector was electrically coupled with an aluminum tube, by a
103 conductive carbon paste. Aluminum was previously polished with different grade emery paper,
104 washed with distilled water and rinsed ultrasonically in pure acetone. Then, the copper-aluminum
105 couple was immersed in an electrolytic solution containing CuSO_4 0.1M and boric acid 0.05M with
106 pH 2 adjusted by sulfuric acid. This galvanic couple leads to dissolution of aluminum, that acts as
107 sacrificial anode, and the simultaneous deposition of Cu into the polycarbonate pores. After
108 nanowires deposition, samples were etched in pure dichloromethane in order to dissolve the
109 template.

110 Morphology was analyzed by scanning electron microscopy (SEM), using a FEI FEG-
111 ESEM (mod. QUANTA 200) equipped with an Energy Dispersive Spectroscopy (EDS) detector. X-
112 ray diffraction was carried out using a RIGAKU diffractometer (model: D-MAX 25600 HK). All
113 diffraction patterns were obtained in the 2θ range from 10° to 100° with a step of 0.004° and a
114 measuring time of 0.067 s for step, using the copper $\text{K}\alpha$ radiation. Diffraction patterns were
115 analyzed by comparison with ICDD database (International Centre for Diffraction Data, card
116 number: Cu 4-836, Au 4-784; AgCl 06-048).

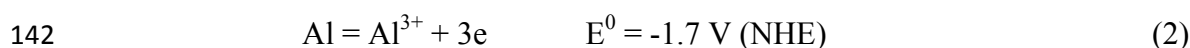
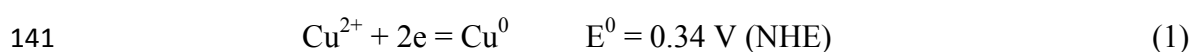
117 For the sensor performance study, nanostructured electrodes were assembled with a copper
118 tape and insulated with a lacquer to have a geometric area of about 0.05 cm^2 . Electrochemical tests
119 were carried out in de-aerated (by N_2 purging) aqueous solutions of 0.1 M NaSO_4 at different pH
120 (adjusted by sulfuric acid), using a three-electrode cell with Ag/AgCl reference electrode and a Pt
121 mesh as counter electrode. Cyclic voltammetry (CV) was carried out with a scan rate of 50 mV/s in
122 the potential range from -1.4 to -0.1 V vs Ag/AgCl. The effect of solution pH on the sensor
123 performance was studied, by testing different solutions (50 ppm of nitrate). Similarly, the effect of
124 surface area was tested by using electrodes consisting of Cu thin film and Cu-NWs of different
125 length (obtained by changing the GD time in the range from 30 to 120 minutes). Sensor calibration

126 curves were obtained by means of LSV carried out in the potential range from -0.1 to -0.8 V
127 (Ag/AgCl) with a scan rate of 10 mV/s, by adding different amount of a standard solution of
128 sodium nitrate to the blank. Selectivity tests were carried out in the presence of copper, lead,
129 nickel, zinc, aluminum, mercury, chorine, potassium, sodium, sulfite, carbonate and magnesium at
130 four different concentrations (0.5, 5, 50 and 500 ppm), in the presence of 50 ppm of nitrate ions.
131 These concentrations are an order of magnitude lower and higher than interfering species,
132 respectively. All the experiments have been repeated at least 3 times.

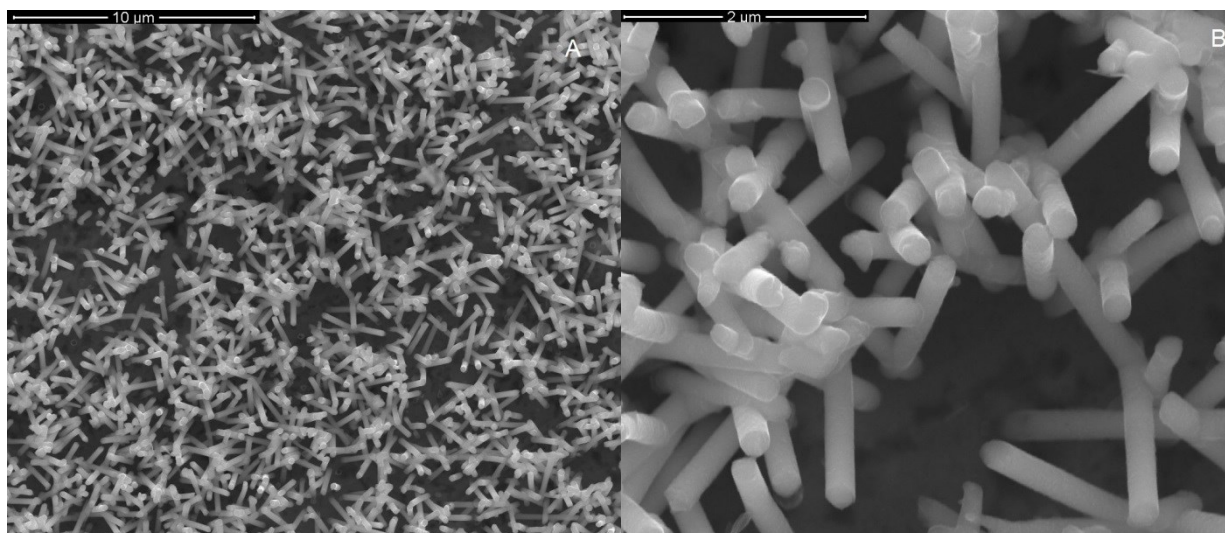
133 **3. Results and discussion**

134 ***3.1 Copper nanowire fabrication***

135 The deposition of copper NWs has been carried out by GD. This process can be controlled by
136 adjusted different parameters such as composition and pH of deposition bath, anodic to cathodic
137 area ratio and deposition time [49], [56]. It is a simple process that allows fabrication of
138 nanostructured materials with different morphology like NWs, NTs and NPs [51], [57]. Following
139 the results obtained in our previous work [44] the growth of Cu NWs inside the pore of the template
140 is due to the following reactions:



143 In particular the dissolution of aluminum anode produces the electrons necessary to the reduction of
144 copper ions. This is a spontaneous process that not requires an external power supply, and in fact,
145 the electromotive force of this process ($\xi = E^0_{\text{cat}} - E^0_{\text{an}}$) is positive leading to an overall negative
146 Gibbs free energy ($\Delta G = -nF\xi$). Figure 1 shows the SEM images of the as prepared Cu nanowires
147 obtained after a deposition time of 30 min and after template dissolution. The typical morphology of
148 nanowires, consisted of interconnected cylindrical wires, obtainable by template deposition in
149 polycarbonate membrane can be observed [49], [44], [58].

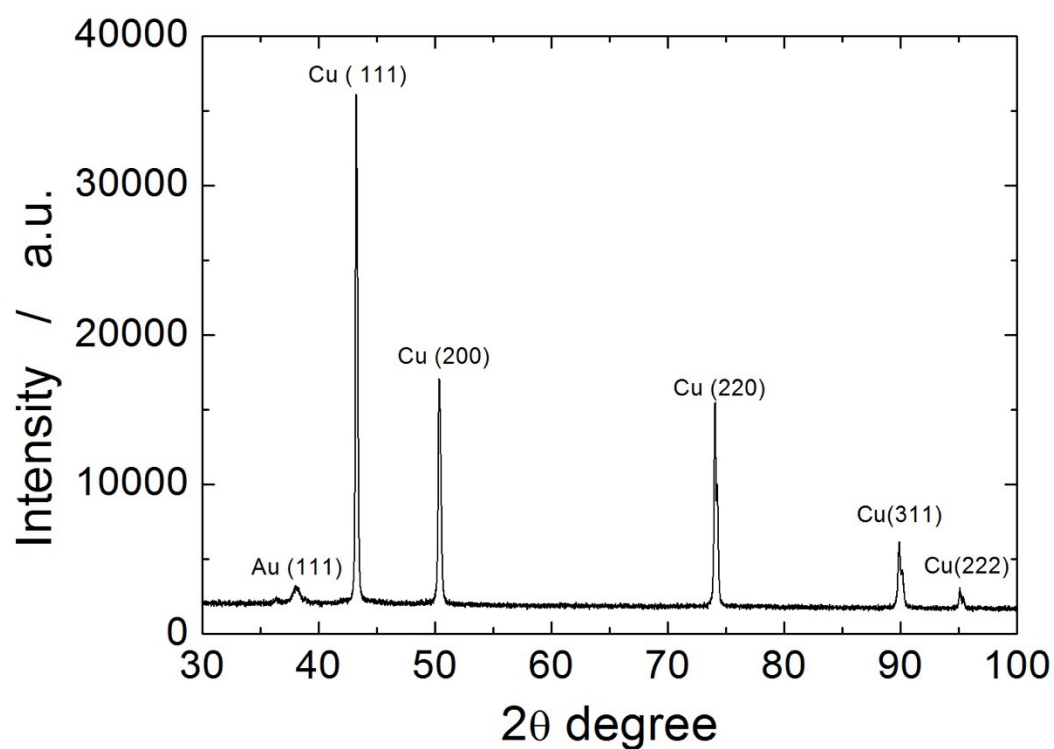


150

151

Figure 1 SEM images of Cu-NWs obtained after 30 minutes of deposition

152



153

154

Figure 2 XRD pattern of as-prepared Cu NWs after template dissolution

155

156

The NWs length increases with increasing the deposition time, particularly, it moves from

157

1.38 ± 0.19 μm after 30 min of deposition to 2.65 ± 0.37 μm after 120 min (Figure S2). NWs have

158 an average diameter of about 220 nm (Figure S3a) according to the nominal mean diameter of the
159 pores of polycarbonate template. In order to fully characterize the nanostructured electrode, XRD
160 (Figure 2) and EDS (Figure S3b) analyses were also carried out.

161 By EDS analysis (Figure S3-b), the presence of copper, arising from both the NWs and current
162 collector, sputtered gold and trace of carbon and oxygen due to residual polycarbonate, was found.
163 Figure 2 shows the XRD pattern of the Cu-NWs electrode and the peaks correspond to a cubic
164 phase of copper can be observed. Also, the main peak of gold, from sputtered gold, was identified.
165 Similar XRD patterns and EDS spectra were obtained for all samples regardless of the deposition
166 time. Thus, from these results it is possible to conclude that GD process led to the formation of pure
167 copper nanowires with a polycrystalline structure.

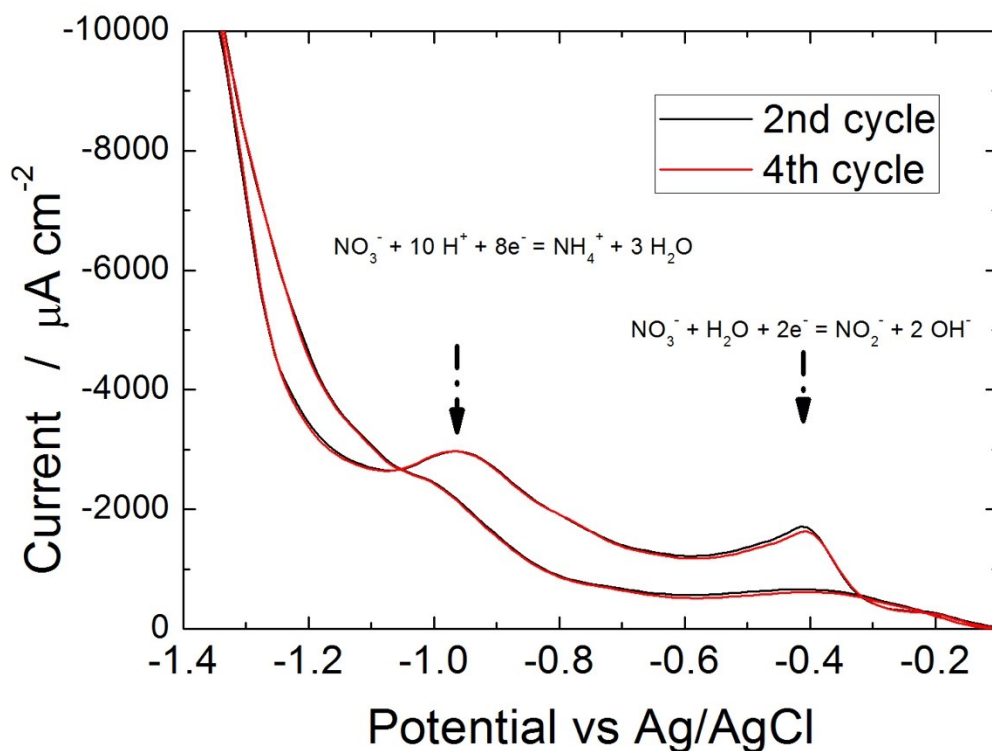
168 **3.2 Electrochemical tests: optimization and calibration**

169 Electrochemical reduction of nitrate ions involves different redox reactions. Davis et al. [39], using
170 a copper based electrode to detect nitrates and nitrites, have found a peak at about -0.46 V Ag/AgCl
171 that is imputable to the reduction of nitrate to nitrite. A similar result was found by other researchers
172 [59–61]. Other studies found a second peak at more cathodic potential (about -0.86 V Ag/AgCl)
173 that was ascribed to the reduction of nitrate ions to ammonia [62,63]. Starting from these literature
174 data, CV analyses were carried out using the as prepared Cu NWs as working electrode using the
175 blank solution (Na_2SO_4 0.1M at pH 2.5) added with NaNO_3 1mM (Figure 3). The CV curves of
176 Figure 3 shows the presence of both the reduction peaks (at about -0.97 V and -0.42 V Ag/AgCl)
177 above described. The peak at -0.42 V has the higher intensity and so sensors were calibrated using
178 this reduction peak.

179 In order to maximize the peak current, the effect of pH of the detection solution was
180 checked. In fact, pH is a crucial parameter to preserve copper metal from oxidation [64] that would
181 result a short life time of Cu based electrode. To overcome this problem, the use of acidic media is

182 strongly recommended [24]; [65]; [66]. But, considering that at low pH also the parasitic reaction of
183 hydrogen evolution occurs, it is necessary to find the best value.

184

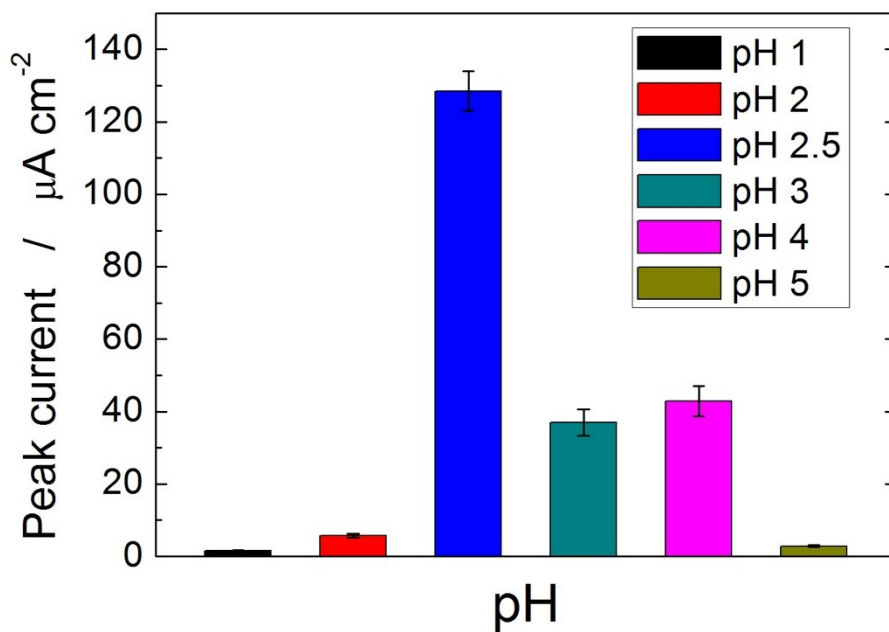


185

186 **Figure 3** CV in the presence of 1mM of nitrate ions using Cu NWs electrode

187

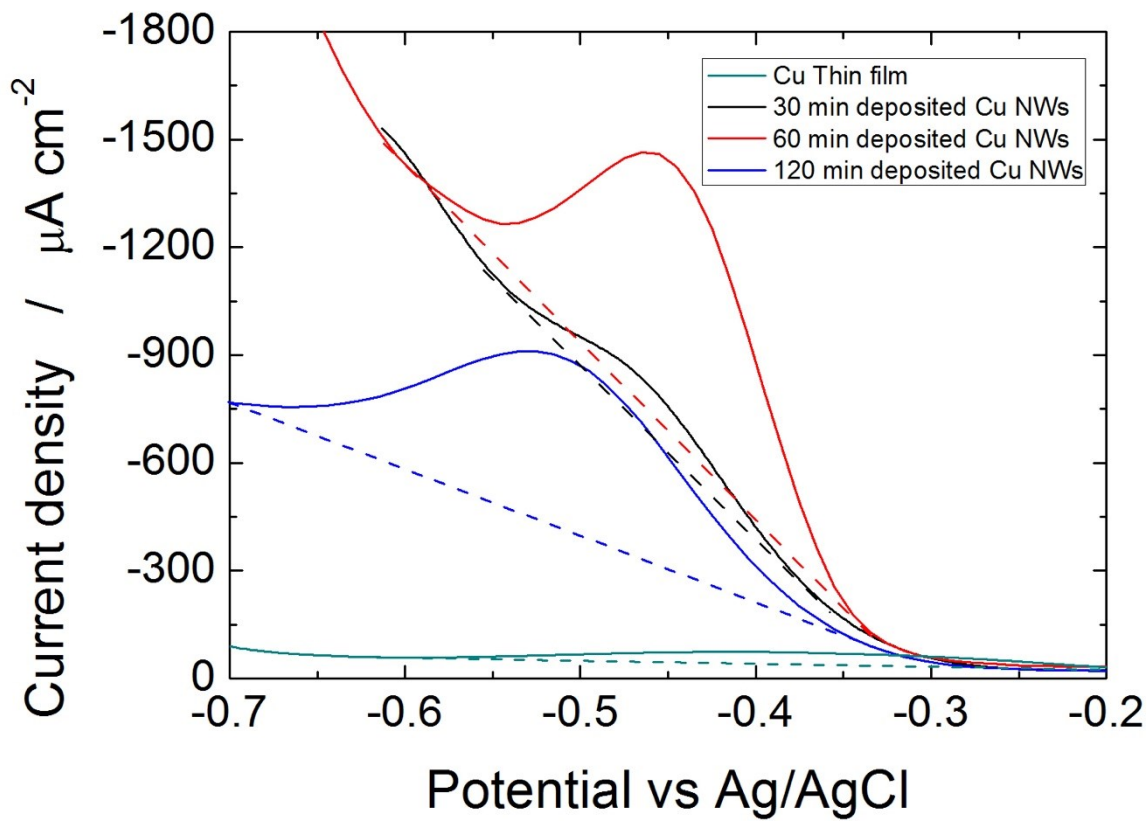
188 Figure 4, shows the effect of pH on the peak current of 3.5 ppm of nitrate using the Cu NWs
189 electrodes. When using a testing solution at $\text{pH} \geq 3$ the copper electrode changes its color after few
190 analyses, shifting from a pink color to a darker one, indicating the copper oxidation, this led to the
191 decrease of peak current clearly observable in figure 4. For $\text{pH} \geq 5$ the oxidation phenomena almost
192 completely hindered the detection of nitrate ions. The detection at $\text{pH} \leq 2$ is minimal due to the
193 presence of hydrogen evolution reaction. The best pH value that we have found is 2.5 that lead to
194 obtain a maximum peak current ($130 \mu\text{A cm}^{-2}$).



195

196

Figure 4 Effect of solution pH on the peak current of the detection of 3.5 ppm of nitrate ions



197

198

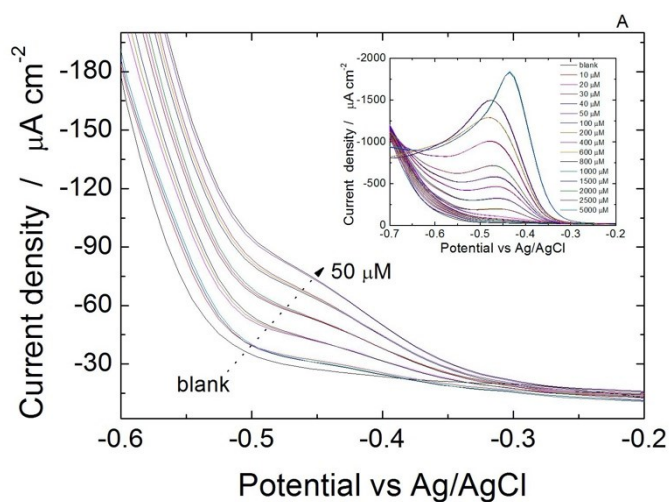
Figure 5 Effect of nanostructures length on the intensity of peak current of nitrate ions detection

199 Figure 5 shows the effect of NWs length on the peak current of 1mM nitrates in a solution of
200 Na_2SO_4 0.1M at pH 2.5. For comparison, also a copper thin film was tested. From a planar electrode
201 to a nanostructured one, the peak current highly increases due to the increase in surface area. If the
202 NWs length is increased (by increasing the deposition time) from 30 min to 60 min the peak current
203 increased as well, showing again the associated effect of the surface area. Interestingly, if the
204 detection of nitrate ions is tried with longer NWs (120 min of deposition), the peak current
205 decreases. We think that this is an effect of wettability. Indeed, vertically standing NWs are quite
206 hydrophobic [67] and the hydrophobicity increases with increasing NW length. Furthermore, this
207 effect is of importance when using polycarbonate as template because these membranes have many
208 pores interconnections. These pores interconnections decrease the NWs wettability due to a higher
209 physical obstruction. We found that in Poretics polycarbonate template (Figure S1), several
210 interconnections are present, at different points of the cross-section of membrane, mainly located
211 between 2 (from the bottom) and 5 μm . Therefore, nanowires that have lengths close to
212 interconnections, such as those obtained after 120 minutes of deposition, even if they are longer
213 than those obtained with a shorter deposition time, do not exhibit a real increase in the surface area.
214 As is clearly visible in Figure S2, these nanowires have a more compact structure. In fact, as the
215 height increases, the empty spaces between the nanowires decrease, making the structure more and
216 more hydrophobic [68]. These results agree with the results of Figure 5 and justify the decrease in
217 peak intensity.

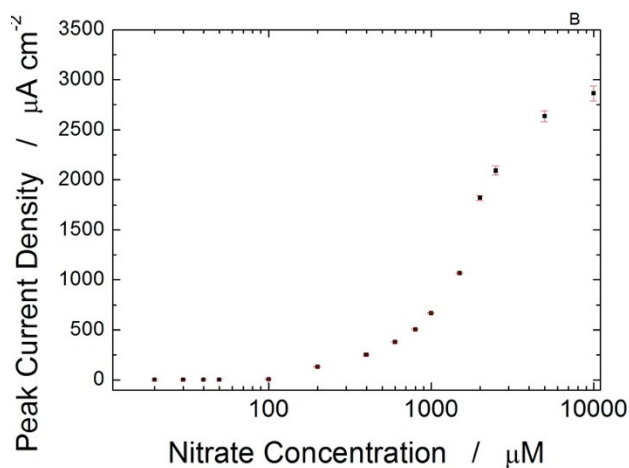
218 The effect of increasing nitrate concentration is shown in Figure 6a. In order to show, at the same
219 time, the reproducibility of the sensor, the LSV curves recorded at increasing concentration, from
220 10 to 50 μM , were repeated in triplicate. For the same concentration value, the LSV curves are
221 almost superimposed (independently of the concentration value) on each other. Thus, it can be
222 concluded, that the electrodes are highly reproducible with a standard deviation of about 7%. The
223 inset of Figure 6a shows the LSV curves for concentration from 100 to 5000 μM . In Figure 6b the

224 corresponding calibration curve, in the entire investigated concentration range, is reported. As can
225 be see, the shape of the calibration curve is a sigmoid with two identifiable linear ranges, the first
226 with low sensitivity ($0.063 \mu\text{A cm}^{-2}$, Figure 4c) and a the second with higher sensitivity ($0.73 \mu\text{A}$
227 cm^{-2}), Figure 4d). After, a final saturation range can be also foreseen. Fernandez-Ramos et al, found
228 a similar behavior when developing a photometric sensor for nitrates [69]. By the way, this is a
229 common behavior of chemical, optical [70–72] and electrochemical sensors [73–77].

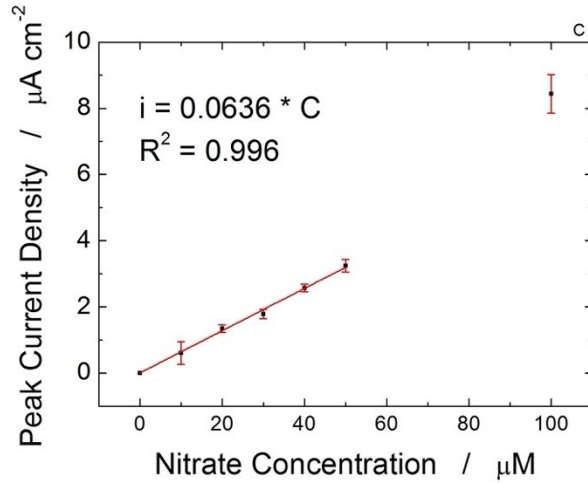
230



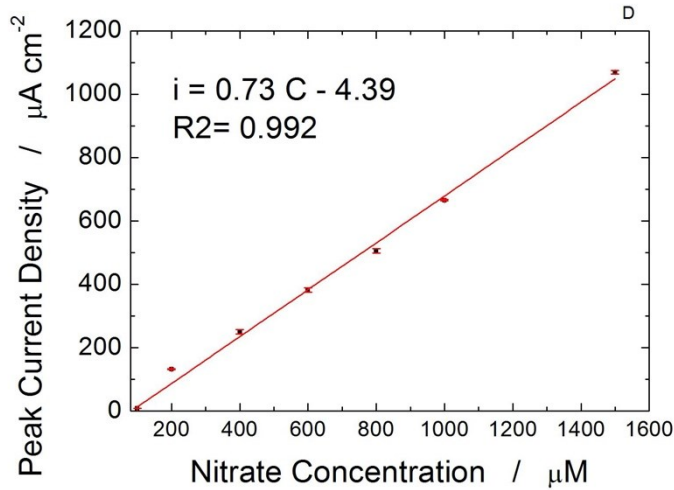
231



232



233



234

235 **Figure 6** Effect of increasing nitrate ions concentration using Cu NWs electrode obtained with 60
 236 min of galvanic deposition

237

238 The LOD was calculated using the following equation:

239
$$\text{LOD} = 3.3 * \text{SD} / \text{S} \quad (3)$$

240 where SD is the standard error of the blank and S the sensitivity of the first linear range. The
 241 calculated LOD is 9.1 μM , that is comparable to value reported in the literatures (see Table S1,
 242 where the performance of most recent electrochemical sensors for nitrate ions detection were
 243 listed). A lower LOD was found by [78] using unsorted thermal annealed Cu nanowires and by
 244 Stortini et al. [55] using ordered electrodeposited nanowire array. In both approaches, differential

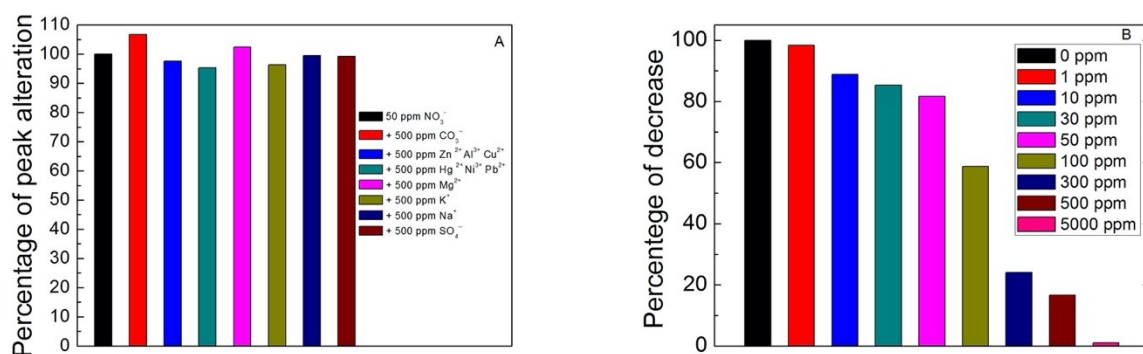
245 pulse voltammetry (DPV) was employed as detection technique. DPV is a more precise
246 electrochemical method but, in comparison to LSV, it is also more complex to optimize in terms of
247 parameters (length of pulse, time duration, ecc) [79]. It is important to note that the LOD here
248 obtained herein, is much lower than the limits established by EPA and WHO (750 μM) and thus
249 higher precision of sensors is useful but not essential. In addition, our electrodes were made with a
250 very low-cost technique, rapidly and without any expensive post-treatment, such as the annealing at
251 high temperature.

252 **3.3 Interference study**

253 In order to fully determine the performance of an electrochemical sensor, it is of great importance to
254 undertake an interference study. It is well known that the presence of other chemicals can interfere
255 with the detection due to both electrode modification and/or for possible voltametric peaks
256 overlapping. Since the aim of this work is to detect nitrates in water real samples, the interfering
257 chemical species (calcium, magnesium, potassium, chlorine, heavy metals, carbonate ions) were
258 chosen as they typically present in water. These chemicals were added to the testing solution at
259 different concentrations (in a very wide range from 0.5 to 500 ppm) and the results are shown in
260 Figure 7a. In a solution of 50 ppm of nitrates, the addition of 500 ppm of interference species
261 (Mg^{2+} , CO_3^{2-} , Cu^{2+} , Pb^{2+} , Zn^{2+} , Ni^{2+} , Hg^{2+} , Al^{3+} , SO_4^{2-} , Na^+) causes a negligible effect. In fact, the
262 peak current density measured in the presence of the only nitrate ions exhibited a variation of lower
263 than 5%. Among the investigated interfering chemical species, the higher interference comes from
264 carbonate ions (about 5%). Finally, it is important to highlight that is very unusual to find 500 ppm
265 of these chemical species in real water samples.

266 A considerable interference effect was found when trying to detect nitrates in presence of chlorine
267 ions. This behavior is consistent with literature data [39,65,66,80] and is probably due to the fouling
268 of sensor surface because of the formation of a thin layer of copper chloride [81]. In fact, it was
269 found that as little as 10 ppm of Cl^- decreases the peak intensity of nitrates by about 10% and peak

270 intensity continued to decrease with increasing Cl^- concentration. This is thus a serious problem for
 271 detection of nitrates in real samples, because chlorine ions are always present in water. In particular,
 272 chlorine concentration is more than 10,000 ppm in sea water, among 50 and 450 ppm in river water
 273 and about 10 ppm in drinking water [81] . In order to overcome this problem, chlorine ions must be
 274 removed. A simple method to remove chlorine is the addition of a silver compound into the solution
 275 to form silver chloride (among the chlorine compounds it is the one with very low solubility). In
 276 fact, the solubility of AgCl is lower than 0.1 ppm [85] and therefore if an appropriate amount of a
 277 silver compound (as Ag_2SO_4) is added to the solution, its chemical precipitation occurs. By adding
 278 silver sulphate, we have obtained a purple precipitate, that was examined by XRD and EDS
 279 (Figure S4), confirming the chemical composition of AgCl . It is important to highlight that, due to
 280 the solubility of silver sulfate (15 mM [85]), this compound can be used to precipitate up to 1000
 281 ppm of chlorine. If the testing solution contains higher concentration of chlorine (as the sea water),
 282 the procedure has to be slightly modified by first adding lead carbonate, in order to precipitate
 283 PbCl_2 . Since the solubility of lead chloride is about 1000 ppm, after its precipitation, it is possible to
 284 eliminate the remaining part of chlorine by adding silver sulfate. The possibility that traces of silver
 285 or lead ions contaminant the samples to test is not a problem because (as showed in Figure S5 for
 286 silver, and in Figure 7 for lead) their presence influences very little the detection of nitrate ions.

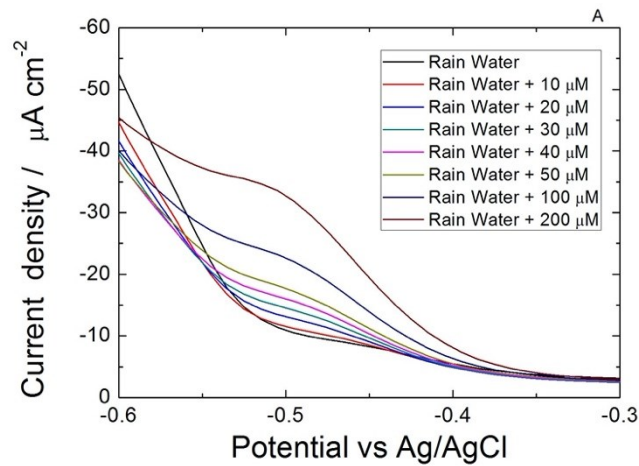


287

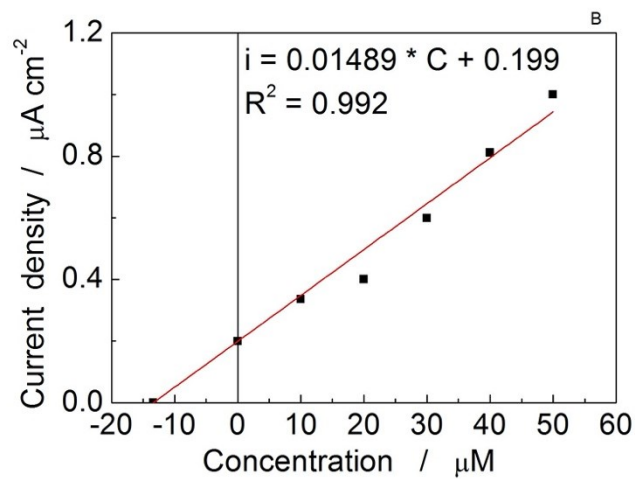
288 **Figure 7** (a) Interference of 500 ppm of different chemical species (b) interference of chlorine on
 289 the peak current for the detection of 50 ppm of nitrate ions

290 **3.4 Real sample analysis**

291 In order to validate the sensors with real sample, 3 different water samples were tested: rain water
292 (Figure 8), river water (from Oreto River, Palermo, Sicily, Italy) and drinking water (Italy,
293 commercial water). The method used to quantify the nitrate concentration is the standard addition
294 method (SAM). Using this technique, no calibration lines are needed because it takes into account
295 the effect of the matrix [86,87].



296



297

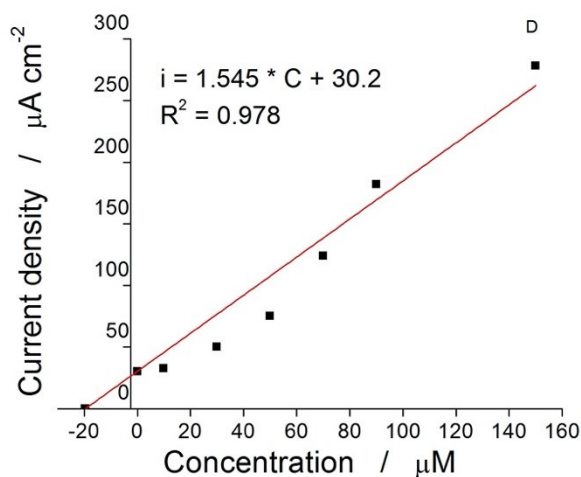
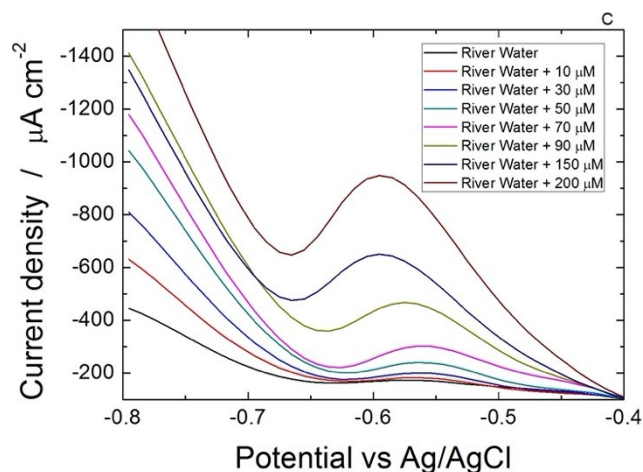


Figure 8 Real samples analysis. (a-b) Rain water (c-d) water from Oreto river.

298

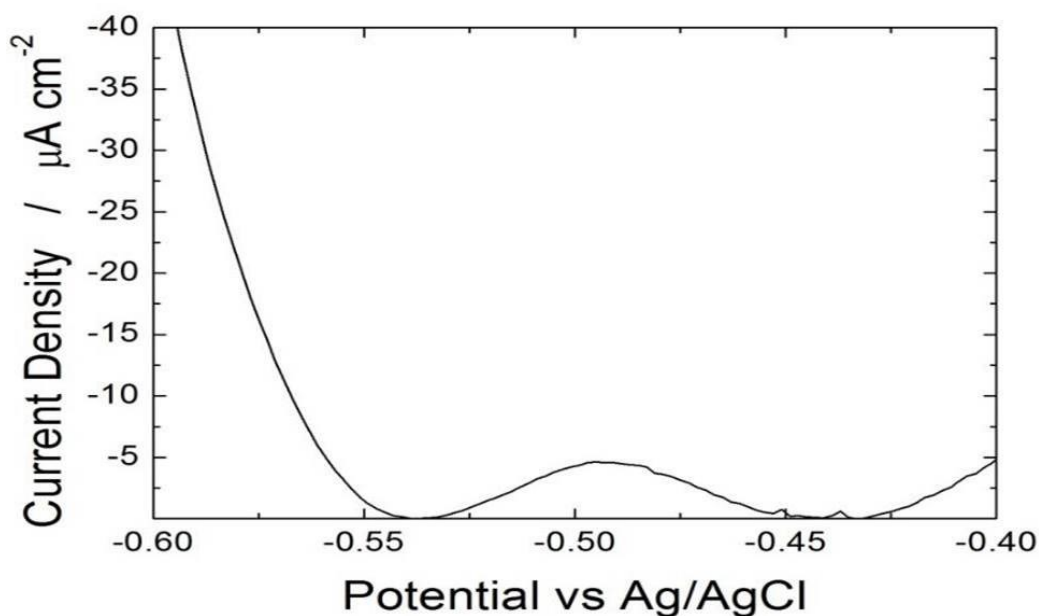
299

300

301

302 Figure 8a shows the analysis carried out using rain water and the effect of increasing concentration
 303 of nitrates. Using the standard addition method (Figure 8b), a nitrate concentration of about 12 μM
 304 (0.7 ppm) was detected using equation 3. Water from Oreto river was collected and filtered through
 305 paper filter and then acidified using sulfuric acid. If this water sample is tested without any other
 306 purification step, no results in terms of nitrates detection are obtained. In fact, using a standard
 307 sodium nitrate solution, the peak of reduction of nitrate ions was not detected even at high
 308 concentration (up to 5 mM), probably due to the high content of chlorine in this real sample (Figure
 309 S6). Thus, water from Oreto was treated by adding silver sulfate in order to remove the chlorine
 310 ions. In particular, silver sulfate was added in different steps (for each step an amount of Ag_2SO_4 to

311 reach a 0.1 mM was used) until to obtain the conclusion of the precipitation of AgCl. After this
312 chemical treatment, the sample was tested and the results are shown in Figure 7b. The chemical
313 purification makes possible the nitrate detection and we found that the peak current increases when
314 increasing the nitrate concentration (Figure 8c). Using the SAM, a concentration of about 22 μM
315 (1.4 ppm) was detected (Figure 8d).
316 Finally, we have also analyzed samples of drinking water (Italy, commercial water). In this case,
317 since the composition of water is completely known (in Figure S7 the data -sheet of water was
318 reported), these water samples were directly tested and, using the calibration line, we have
319 calculated, from the intensity of the peak current (Figure 9), the corresponding concentration of
320 nitrate ions. The LSV experiment leads to a peak current of about $4.5 \mu\text{A cm}^{-2}$, corresponding to
321 4.38 ppm of nitrate ions (calibration of figure 6C). This value is very close to the value reported in
322 the data-sheet of this commercial drinking water (4.4 ppm, Figure S5) that was measured by
323 conventional laboratory techniques. This result testifying the good behavior of the sensors proposed
324 in this work.



325

326

Figure 9 LSV experiment carried out with commercial drinking water

327

328 **Conclusion**

329 Copper NWs was fabricated by galvanic deposition and successfully used as nitrates sensor. The
330 use of galvanic method makes the electrode fabrication cheap, fast, reproducible and easy to carry
331 out. The NWs length can be controlled by tuning the deposition time and the effect of surface area
332 on the features of nitrates sensor is shown. The sensor was optimized in terms NWs length and pH
333 of solution detection. In the best conditions a LOD of about 9 μM was found. Two linear ranges
334 were found, from 10 to 50 μM and 50 to 1500 μM , with a sensitivity of 0.0636 and 0.73 $\mu\text{A } \mu\text{M}^{-1}$
335 cm^{-2} , respectively. Selectivity tests showed that the sensor is highly selective towards many
336 chemical species, typical present in real water samples, but as aspect, the presence of chlorine ions
337 interferes with nitrates detection even at low concentration. In order to overcome this problem an
338 easy and fast procedure is described to make chlorine precipitate. The sensor was validated using
339 real water sample such as rain, river and drinkable water showing the applicability of the proposed
340 electrode.

341

342 **Bibliography**

- 343 [1] M. Ward, R. Jones, J. Brender, T. de Kok, P. Weyer, B. Nolan, C. Villanueva, S. van Breda,
344 Drinking Water Nitrate and Human Health: An Updated Review, *Int. J. Environ. Res. Public. Health.* 15
345 (2018) 1557. <https://doi.org/10.3390/ijerph15071557>.
- 346 [2] Md.E.E. Alahi, S.C. Mukhopadhyay, Detection methods of nitrate in water: A review, *Sens.*
347 *Actuators Phys.* 280 (2018) 210–221. <https://doi.org/10.1016/j.sna.2018.07.026>.
- 348 [3] T. Öznülür, B. Özdurak, H. Öztürk Doğan, Electrochemical reduction of nitrate on graphene
349 modified copper electrodes in alkaline media, *J. Electroanal. Chem.* 699 (2013) 1–5.
350 <https://doi.org/10.1016/j.jelechem.2013.04.001>.
- 351 [4] N.S. Bryan, J. Loscalzo, Nitrite and nitrate in human health and disease, 2017.
352 <http://dx.doi.org/10.1007/978-3-319-46189-2> (accessed January 14, 2020).
- 353 [5] C.S. Bruning-Fann, J.B. Kaneene, The effects of nitrate, nitrite and N-nitroso compounds on human
354 health: a review, *Vet. Hum. Toxicol.* 35 (1993) 521–538.
- 355 [6] W. Lijinsky, N-Nitroso compounds in the diet, *Mutat. Res. Toxicol. Environ. Mutagen.* 443 (1999)
356 129–138. [https://doi.org/10.1016/S1383-5742\(99\)00015-0](https://doi.org/10.1016/S1383-5742(99)00015-0).

- 357 [7] European Food Safety Authority, Nitrate in vegetables Scientific Opinion of the Panel on
358 Contaminants in the Food chain, *EFSA J.* 689 (2008) 1–79.
- 359 [8] Y.H. Loh, P. Jakszyn, R.N. Luben, A.A. Mulligan, P.N. Mitrou, K.-T. Khaw, N-nitroso compounds
360 and cancer incidence: the European Prospective Investigation into Cancer and Nutrition (EPIC)–Norfolk
361 Study, *Am. J. Clin. Nutr.* 93 (2011) 1053–1061. <https://doi.org/10.3945/ajcn.111.012377>.
- 362 [9] S.S. Mirvish, Role of N-nitroso compounds (NOC) and N-nitrosation in etiology of gastric,
363 esophageal, nasopharyngeal and bladder cancer and contribution to cancer of known exposures to NOC,
364 *Cancer Lett.* 93 (1995) 17–48. [https://doi.org/10.1016/0304-3835\(95\)03786-V](https://doi.org/10.1016/0304-3835(95)03786-V).
- 365 [10] D.B.J. Bosnir, M. Bevardi, A.G. Boskovic, S.M.D. Lasic, A. Krivohlavek, A. Racs, A. Mojosovic-
366 Cuic, N.U. Trstenjak, NITRATE IN LEAFY GREEN VEGETABLES AND ESTIMATED INTAKE, *Afr. J.*
367 *Tradit. Complement. Altern. Med.* 14 (2017) 31–41. <https://doi.org/10.21010/ajtcam.v14i3.4>.
- 368 [11] L. Knobeloch, B. Salna, A. Hogan, J. Postle, H. Anderson, Blue babies and nitrate-contaminated
369 well water., *Environ. Health Perspect.* 108 (2000) 675–678. <https://doi.org/10.1289/ehp.00108675>.
- 370 [12] <https://www.epa.gov/ground-water-and-drinking-water/national-primary-drinking-water-regulations>,
371 (n.d.).
- 372 [13] M. Moorcroft, Detection and determination of nitrate and nitrite: a review, *Talanta.* 54 (2001) 785–
373 803. [https://doi.org/10.1016/S0039-9140\(01\)00323-X](https://doi.org/10.1016/S0039-9140(01)00323-X).
- 374 [14] J.C. Suggs, J.H. Margeson, M.R. Midgett, Reduction of Nitrate to Nitrite with Cadmium, *Anal.*
375 *Chem.* 52 (1980) 1955–1957.
- 376 [15] N.R. Stradiotto, H. Yamanaka, M.V.B. Zanoni, Electrochemical sensors: a powerful tool in
377 analytical chemistry, *J. Braz. Chem. Soc.* 14 (2003) 159–173. <https://doi.org/10.1590/S0103-50532003000200003>.
- 379 [16] U. Yogeswaran, S.-M. Chen, A Review on the Electrochemical Sensors and Biosensors Composed
380 of Nanowires as Sensing Material, *Sensors.* 8 (2008) 290–313. <https://doi.org/10.3390/s8010290>.
- 381 [17] P. Dardano, I. Rea, L. De Stefano, Microneedles based electrochemical sensors: new tools for
382 advanced biosensing, *Curr. Opin. Electrochem.* (2019) S2451910319300602.
383 <https://doi.org/10.1016/j.coelec.2019.05.012>.
- 384 [18] Carmelo Sunseri, Cristina Cocchiara, Fabrizio Ganci, Alessandra Moncada, Roberto Luigi Oliveri,
385 Bernardo Patella, Salvatore Piazza, Rosalinda Inguanta, Nanostructured electrochemical devices for sensing,
386 energy conversion and storage, *Chem. Eng. Trans.* 47 (2016) 43–48. <https://doi.org/10.3303/CET1647008>.
- 387 [19] Patella B., Piazza S., Sunseri C., Inguanta R., Nio thin film for mercury detection in water by square
388 wave anodic stripping voltammetry, *Chem. Eng. Trans.* 60 (2017) 1–6. <https://doi.org/10.3303/CET1760001>.
- 389 [20] A.J.C. Wahl, I.P. Seymour, M. Moore, P. Lovera, A. O’Riordan, J.F. Rohan, Diffusion profile
390 simulations and enhanced iron sensing in generator-collector mode at interdigitated nanowire electrode
391 arrays, *Electrochimica Acta.* 277 (2018) 235–243. <https://doi.org/10.1016/j.electacta.2018.04.181>.
- 392 [21] W.-O. Caron, M. Lamhamedi, J. Viens, Y. Messaddeq, Practical Application of Electrochemical
393 Nitrate Sensor under Laboratory and Forest Nursery Conditions, *Sensors.* 16 (2016) 1190.
394 <https://doi.org/10.3390/s16081190>.

- 395 [22] S. Zhao, J. Tong, Y. Li, J. Sun, C. Bian, S. Xia, Palladium-Gold Modified Ultramicro Interdigital
396 Array Electrode Chip for Nitrate Detection in Neutral Water, *Micromachines*. 10 (2019) 223.
397 <https://doi.org/10.3390/mi10040223>.
- 398 [23] G.A. Sherwood, D.C. Johnson, A chromatographic determination of nitrate with amperometric
399 detection at a copperized cadmium electrode, *Anal. Chim. Acta*. 129 (1981) 101–111.
400 [https://doi.org/10.1016/S0003-2670\(01\)84123-4](https://doi.org/10.1016/S0003-2670(01)84123-4).
- 401 [24] M. Bertotti, D. Pletcher, Amperometric determination of nitrite via reaction with iodide using
402 microelectrodes, *Anal. Chim. Acta*. 337 (1997) 49–55. [https://doi.org/10.1016/S0003-2670\(96\)00431-X](https://doi.org/10.1016/S0003-2670(96)00431-X).
- 403 [25] A.Y. Chamsi, A.G. Fogg, Oxidative flow injection amperometric determination of nitrite at an
404 electrochemically pre-treated glassy carbon electrode, *The Analyst*. 113 (1988) 1723.
405 <https://doi.org/10.1039/an9881301723>.
- 406 [26] S.A. Glazier, E.R. Campbell, W.H. Campbell, Construction and Characterization of Nitrate
407 Reductase-Based Amperometric Electrode and Nitrate Assay of Fertilizers and Drinking Water, *Anal. Chem.*
408 70 (1998) 1511–1515. <https://doi.org/10.1021/ac971146s>.
- 409 [27] M.A. Alawi, Determination of nitrate and nitrite in water by HPLC with amperometric detection,
410 (n.d.) 1.
- 411 [28] D. Pan, W. Lu, H. Zhang, L. Zhang, J. Zhuang, Voltammetric determination of nitrate in water
412 samples at copper modified bismuth bulk electrode, *Int. J. Environ. Anal. Chem.* 93 (2013) 935–945.
413 <https://doi.org/10.1080/03067319.2012.690149>.
- 414 [29] J. Krista, M. Kopanica, L. Novotny, Voltammetric Determination of Nitrates Using Silver
415 Electrodes, (2000) 6.
- 416 [30] M.E. Bodini, D.T. Sawyer, Voltammetric determination of nitrate ion at parts-per-billion levels,
417 *Anal. Chem.* 49 (1977) 485–489. <https://doi.org/10.1021/ac50011a037>.
- 418 [31] R.J. Davenport, D.C. Johnson, Voltammetric determination of nitrate and nitrite ions using a rotating
419 cadmium disk electrode, *Anal. Chem.* 45 (1973) 1979–1980. <https://doi.org/10.1021/ac60333a038>.
- 420 [32] S.M. Shariar, T. Hinoue, Simultaneous Voltammetric Determination of Nitrate and Nitrite Ions
421 Using a Copper Electrode Pretreated by Dissolution/Redeposition, *Anal. Sci.* 26 (2010) 1173–1179.
422 <https://doi.org/10.2116/analsci.26.1173>.
- 423 [33] V. Mareček, H. Jänchenová, Z. Samec, M. Březina, Voltammetric determination of nitrate,
424 perchlorate and iodide at a hanging electrolyte drop electrode, *Anal. Chim. Acta*. 185 (1986) 359–362.
425 [https://doi.org/10.1016/0003-2670\(86\)80067-8](https://doi.org/10.1016/0003-2670(86)80067-8).
- 426 [34] D. Quan, J.H. Shim, J.D. Kim, H.S. Park, G.S. Cha, H. Nam, Electrochemical Determination of
427 Nitrate with Nitrate Reductase-Immobilized Electrodes under Ambient Air, *Anal. Chem.* 77 (2005) 4467–
428 4473. <https://doi.org/10.1021/ac050198b>.
- 429 [35] D. Albanese, M. Di Matteo, C. Alessio, Screen printed biosensors for detection of nitrates in
430 drinking water, in: *Comput. Aided Chem. Eng.*, Elsevier, 2010: pp. 283–288. [https://doi.org/10.1016/S1570-7946\(10\)28048-3](https://doi.org/10.1016/S1570-7946(10)28048-3).
- 432 [36] A.A. Gokhale, J. Lu, R.R. Weerasiri, J. Yu, I. Lee, Amperometric Detection and Quantification of
433 Nitrate Ions Using a Highly Sensitive Nanostructured Membrane Electrodeposited Biosensor Array,

- 434 Electroanalysis. 27 (2015) 1127–1137. <https://doi.org/10.1002/elan.201400547>.
- 435 [37] M. Badea, A. Amine, G. Palleschi, D. Moscone, G. Volpe, A. Curulli, New electrochemical sensors
436 for detection of nitrites and nitrates, *J. Electroanal. Chem.* 509 (2001) 66–72. [https://doi.org/10.1016/S0022-](https://doi.org/10.1016/S0022-0728(01)00358-8)
437 0728(01)00358-8.
- 438 [38] D. Reyter, Electrochemical Reduction of Nitrate, in: G. Kreysa, K. Ota, R.F. Savinell (Eds.), *Encycl.*
439 *Appl. Electrochem.*, Springer New York, New York, NY, 2014: pp. 585–593. [https://doi.org/10.1007/978-1-](https://doi.org/10.1007/978-1-4419-6996-5_135)
440 4419-6996-5_135.
- 441 [39] J. Davis, M.J. Moorcroft, S.J. Wilkins, R.G. Compton, M.F. Cardosi, Electrochemical detection of
442 nitrate and nitrite at a copper modified electrode, *The Analyst.* 125 (2000) 737–742.
443 <https://doi.org/10.1039/a909762g>.
- 444 [40] H. Essousi, H. Barhoumi, M. Bibani, N. Ktari, F. Wendler, A. Al-Hamry, O. Kanoun, Ion-Imprinted
445 Electrochemical Sensor Based on Copper Nanoparticles-Polyaniline Matrix for Nitrate Detection, *J. Sens.*
446 2019 (2019) 1–14. <https://doi.org/10.1155/2019/4257125>.
- 447 [41] H. Bagheri, A. Hajian, M. Rezaei, A. Shirzadmehr, Composite of Cu metal nanoparticles-multiwall
448 carbon nanotubes-reduced graphene oxide as a novel and high performance platform of the electrochemical
449 sensor for simultaneous determination of nitrite and nitrate, *J. Hazard. Mater.* 324 (2017) 762–772.
450 <https://doi.org/10.1016/j.jhazmat.2016.11.055>.
- 451 [42] B. Hafezi, M.R. Majidi, A sensitive and fast electrochemical sensor based on copper nanostructures
452 for nitrate determination in foodstuffs and mineral waters, *Anal. Methods.* 5 (2013) 3552.
453 <https://doi.org/10.1039/c3ay26598f>.
- 454 [43] Y. Wu, M. Gao, S. Li, Y. Ren, G. Qin, Copper wires with seamless 1D nanostructures: Preparation
455 and electrochemical sensing performance, *Mater. Lett.* 211 (2018) 247–249.
456 <https://doi.org/10.1016/j.matlet.2017.10.016>.
- 457 [44] Bernardo Patella, Rosalinda Inguanta, Salvatore Piazza, Carmelo Sunseri, Nanowire ordered arrays
458 for electrochemical sensing of h₂o₂, *Chem. Eng. Trans.* 47 (2016) 19–24.
459 <https://doi.org/10.3303/CET1647004>.
- 460 [45] R. Inguanta, S. Piazza, C. Sunseri, Novel procedure for the template synthesis of metal
461 nanostructures, *Electrochem. Commun.* 10 (2008) 506–509. <https://doi.org/10.1016/j.elecom.2008.01.019>.
- 462 [46] B. Patella, C. Sunseri, R. Inguanta, Nanostructured Based Electrochemical Sensors, *J. Nanosci.*
463 *Nanotechnol.* 19 (2019) 3459–3470. <https://doi.org/10.1166/jnn.2019.16110>.
- 464 [47] F. Ganci, S. Lombardo, C. Sunseri, R. Inguanta, Nanostructured electrodes for hydrogen production
465 in alkaline electrolyzer, *Renew. Energy.* 123 (2018) 117–124. <https://doi.org/10.1016/j.renene.2018.02.033>.
- 466 [48] F. Ganci, T. Baguet, G. Aiello, V. Cusumano, P. Mandin, C. Sunseri, R. Inguanta, Nanostructured Ni
467 Based Anode and Cathode for Alkaline Water Electrolyzers, *Energies.* 12 (2019) 3669.
468 <https://doi.org/10.3390/en12193669>.
- 469 [49] B. Patella, R. Inguanta, S. Piazza, C. Sunseri, A nanostructured sensor of hydrogen peroxide, *Sens.*
470 *Actuators B Chem.* 245 (2017) 44–54. <https://doi.org/10.1016/j.snb.2017.01.106>.
- 471 [50] Fabrizio Ganci, Rosalinda Inguanta, Salvatore Piazza, Carmelo Sunseri, Salvatore Lombardo,
472 Fabrication and characterization of nanostructured ni and pd electrodes for hydrogen evolution reaction (her)

- 473 in water-alkaline electrolyzer, *Chem. Eng. Trans.* 57 (2017) 1591–1596.
474 <https://doi.org/10.3303/CET1757266>.
- 475 [51] M. Battaglia, S. Piazza, C. Sunseri, R. Inguanta, Amorphous silicon nanotubes via galvanic
476 displacement deposition, *Electrochem. Commun.* 34 (2013) 134–137.
477 <https://doi.org/10.1016/j.elecom.2013.05.041>.
- 478 [52] C. Cocchiara, C. Sunseri, S. Piazza, R. Inguanta, Pb-PbOHCl Composite Nanowires Synthesized by
479 Galvanic Deposition in Template, *J. Nanosci. Nanotechnol.* 19 (2019) 4677–4685.
480 <https://doi.org/10.1166/jnn.2019.16362>.
- 481 [53] A. Moncada, S. Piazza, C. Sunseri, R. Inguanta, Recent improvements in PbO₂ nanowire electrodes
482 for lead-acid battery, *J. Power Sources.* 275 (2015) 181–188.
483 <https://doi.org/10.1016/j.jpowsour.2014.10.189>.
- 484 [54] N. Karimian, L. Moretto, P. Ugo, Nanobiosensing with Arrays and Ensembles of Nanoelectrodes,
485 *Sensors.* 17 (2016) 65. <https://doi.org/10.3390/s17010065>.
- 486 [55] A.M. Stortini, L.M. Moretto, A. Mardegan, M. Ongaro, P. Ugo, Arrays of copper nanowire
487 electrodes: Preparation, characterization and application as nitrate sensor, *Sens. Actuators B Chem.* 207
488 (2015) 186–192. <https://doi.org/10.1016/j.snb.2014.09.109>.
- 489 [56] R. Inguanta, G. Ferrara, S. Piazza, C. Sunseri, A new route to grow oxide nanostructures based on
490 metal displacement deposition. Lanthanides oxy/hydroxides growth, *Electrochimica Acta.* 76 (2012) 77–87.
491 <https://doi.org/10.1016/j.electacta.2012.04.146>.
- 492 [57] R. Inguanta, S. Piazza, C. Sunseri, A Route to Grow Oxide Nanostructures Based on Metal
493 Displacement Deposition: Lanthanides Oxy/Hydroxides Characterization, *J. Electrochem. Soc.* 159 (2012)
494 D493–D500. <https://doi.org/10.1149/2.047208jes>.
- 495 [58] M. Battaglia, R. Inguanta, S. Piazza, C. Sunseri, Fabrication and characterization of nanostructured
496 Ni–IrO₂ electrodes for water electrolysis, *Int. J. Hydrog. Energy.* 39 (2014) 16797–16805.
497 <https://doi.org/10.1016/j.ijhydene.2014.08.065>.
- 498 [59] J. Peng, L. Liu, H. Kuang, G. Cui, C. Xu, Development of an icELISA and immunochromatographic
499 strip for detection of norfloxacin and its analogs in milk, *Food Agric. Immunol.* 28 (2017) 288–298.
500 <https://doi.org/10.1080/09540105.2016.1263987>.
- 501 [60] Y. Li, Z. Zhang, Y. Song, C. Bian, J. Sun, H. Dong, S. Xia, Determination of Nitrate in Potable
502 Water Using a Miniaturized Electrochemical Sensor, in: 2018 IEEE 13th Annu. Int. Conf. NanoMicro Eng.
503 Mol. Syst. NEMS, IEEE, Singapore, 2018: pp. 619–622. <https://doi.org/10.1109/NEMS.2018.8557007>.
- 504 [61] A.M. Stortini, S. Fabris, G. Saorin, E.V. Falzacappa, L.M. Moretto, P. Ugo, Plasma Activation of
505 Copper Nanowires Arrays for Electrocatalytic Sensing of Nitrate in Food and Water, *Nanomaterials.* 9
506 (2019) 150. <https://doi.org/10.3390/nano9020150>.
- 507 [62] H.R. Lotfi Zadeh Zhad, R.Y. Lai, Comparison of nanostructured silver-modified silver and carbon
508 ultramicroelectrodes for electrochemical detection of nitrate, *Anal. Chim. Acta.* 892 (2015) 153–159.
509 <https://doi.org/10.1016/j.aca.2015.08.022>.
- 510 [63] N. Aouina, H. Cachet, C. Debiemme-chouvy, T.T.M. Tran, Insight into the electroreduction of
511 nitrate ions at a copper electrode, in neutral solution, after determination of their diffusion coefficient by
512 electrochemical impedance spectroscopy, *Electrochimica Acta.* 55 (2010) 7341–7345.

- 513 <https://doi.org/10.1016/j.electacta.2010.07.032>.
- 514 [64] B. Zhang, B. Chen, J. Wu, S. Hao, G. Yang, X. Cao, L. Jing, M. Zhu, S.H. Tsang, E.H.T. Teo, Y.
515 Huang, The Electrochemical Response of Single Crystalline Copper Nanowires to Atmospheric Air and
516 Aqueous Solution, *Small*. 13 (2017) 1603411. <https://doi.org/10.1002/sml.201603411>.
- 517 [65] D. Pletcher, Z. Poorabedt, The reduction of nitrate at a copper cathode in aqueous acid.pdf,
518 *Electrochimica Acta*. 24 (1979) 1253–1256.
- 519 [66] N.G. Carpenter, D. Pletcher, Amperometric method for the determination of nitrate in water, *Anal.*
520 *Chim. Acta*. 317 (1995) 287–293. [https://doi.org/10.1016/0003-2670\(95\)00384-3](https://doi.org/10.1016/0003-2670(95)00384-3).
- 521 [67] R. Wen, Q. Li, J. Wu, G. Wu, W. Wang, Y. Chen, X. Ma, D. Zhao, R. Yang, Hydrophobic copper
522 nanowires for enhancing condensation heat transfer, *Nano Energy*. 33 (2017) 177–183.
523 <https://doi.org/10.1016/j.nanoen.2017.01.018>.
- 524 [68] Y.-H. Cheng, C.-K. Chou, C. Chen, S.-Y. Cheng, Critical length of nanowires for hydrophobic
525 behavior, *Chem. Phys. Lett.* 397 (2004) 17–20. <https://doi.org/10.1016/j.cplett.2004.08.063>.
- 526 [69] M.D. Fernández-Ramos, M. Greluk, A.J. Palma, E. Arroyo-Guerrero, J. Gómez-Sánchez, L.F.
527 Capitán-Vallvey, The use of one-shot sensors with a dedicated portable electronic radiometer for nitrate
528 measurements in aqueous solutions, *Meas. Sci. Technol.* 19 (2008) 095204. [https://doi.org/10.1088/0957-](https://doi.org/10.1088/0957-0233/19/9/095204)
529 [0233/19/9/095204](https://doi.org/10.1088/0957-0233/19/9/095204).
- 530 [70] G. Mohr, M. Wenzel, F. Lehmann, P. Czerney, A chromoreactand for optical sensing of
531 amphetamines, *Anal. Bioanal. Chem.* 374 (2002) 399–402. <https://doi.org/10.1007/s00216-002-1519-0>.
- 532 [71] A. Lapresta-Fernández, R. Huertas, M. Melgosa, L.F. Capitán-Vallvey, Multianalyte imaging in one-
533 shot format sensors for natural waters, *Anal. Chim. Acta*. 636 (2009) 210–217.
534 <https://doi.org/10.1016/j.aca.2009.01.044>.
- 535 [72] Suherman, M. Kinichi, K. Toshikazu, Highly selective and sensitive detection of β -agonists using a
536 surface plasmon resonance sensor based on an alkanethiol monolayer functionalized on a Au surface.pdf,
537 *Biosens. Bioelectron.* 67 (2015) 356–363.
- 538 [73] M. McMullan, N. Sun, P. Papakonstantinou, M. Li, W. Zhou, D. Mihailovic, Aptamer conjugated
539 Mo6S9-xIx nanowires for direct and highly sensitive electrochemical sensing of thrombin, *Biosens.*
540 *Bioelectron.* 26 (2011) 1853–1859. <https://doi.org/10.1016/j.bios.2010.01.030>.
- 541 [74] H. Lin, H. Cheng, L. Liu, Z. Zhu, Y. Shao, P. Papakonstantinou, D. Mihailović, M. Li, Thionin
542 attached to a gold electrode modified with self-assembly of Mo6S9-XIX nanowires for amplified
543 electrochemical detection of natural DNA, *Biosens. Bioelectron.* 26 (2011) 1866–1870.
544 <https://doi.org/10.1016/j.bios.2010.01.035>.
- 545 [75] Md.A. Kafi, T.-H. Kim, J.H. An, J.-W. Choi, Fabrication of Cell Chip for Detection of Cell Cycle
546 Progression Based on Electrochemical Method, *Anal. Chem.* 83 (2011) 2104–2111.
547 <https://doi.org/10.1021/ac102895b>.
- 548 [76] K. Islam, Y.-C. Jang, K.J. Sandeep, H.L. Hyun, K. Yong-Sang, Microfluidic Biosensor for β -
549 Amyloid(1-42) Detection Using Cyclic Voltammetry, *J. Nanosci. Nanotechnol.* 11 (2011) 5657–5662.
- 550 [77] G. Gauglitz, Analytical evaluation of sensor measurements, *Anal. Bioanal. Chem.* 410 (2018) 5–13.
551 <https://doi.org/10.1007/s00216-017-0624-z>.

- 552 [78] J. Liang, Y. Zheng, Z. Liu, Nanowire-based Cu electrode as electrochemical sensor for detection of
553 nitrate in water, *Sens. Actuators B Chem.* 232 (2016) 336–344. <https://doi.org/10.1016/j.snb.2016.03.145>.
- 554 [79] A.J. Bard, L.R. Faulkner, *Electrochemical methods: fundamentals and applications*, 2nd ed, Wiley,
555 New York, 2001.
- 556 [80] A.G. Fogg, S.P. Scullion, T.E. Edmonds, B.J. Birch, Direct reductive amperometric determination of
557 nitrate at a copper electrode formed in situ in a capillary-fill sensor device, *The Analyst.* 116 (1991) 573.
558 <https://doi.org/10.1039/an9911600573>.
- 559 [81] G. Karim-Nezhad, P. Seyed Dorraji, Copper chloride modified copper electrode: Application to
560 electrocatalytic oxidation of methanol, *Electrochimica Acta.* 55 (2010) 3414–3420.
561 <https://doi.org/10.1016/j.electacta.2010.01.057>.
- 562 [82] EPA Nitrati.pdf, (n.d.). [https://www.epa.gov/ground-water-and-drinking-water/national-primary-](https://www.epa.gov/ground-water-and-drinking-water/national-primary-drinking-water-regulations)
563 [drinking-water-regulations](https://www.epa.gov/ground-water-and-drinking-water/national-primary-drinking-water-regulations).
- 564 [83] R.J. Spencer, H.P. Eugster, B.F. Jones, S.L. Rettig, Geochemistry of Great Salt Lake, Utah I:
565 Hydrochemistry since 1850, *Geochim. Cosmochim. Acta.* 49 (1985) 727–737. [https://doi.org/10.1016/0016-](https://doi.org/10.1016/0016-7037(85)90167-X)
566 [7037\(85\)90167-X](https://doi.org/10.1016/0016-7037(85)90167-X).
- 567 [84] M. Pontié, J.S. Derauw, S. Plantier, L. Edouard, L. Bailly, Seawater desalination: nanofiltration—a
568 substitute for reverse osmosis?, *Desalination Water Treat.* 51 (2013) 485–494.
569 <https://doi.org/10.1080/19443994.2012.714594>.
- 570 [85] R.C. West, *Handbook of chemistry and physics*, 56th ed., 1975.
- 571 [86] J.E.T. Andersen, The standard addition method revisited, *TrAC Trends Anal. Chem.* 89 (2017) 21–
572 33. <https://doi.org/10.1016/j.trac.2016.12.013>.
- 573 [87] B.E.H. Saxberg, B.R. Kowalski, Generalized standard addition method, *Anal. Chem.* 51 (1979)
574 1031–1038. <https://doi.org/10.1021/ac50043a059>.
- 575
- 576

577 **Figure Captions**

578

579 **Figure 8** SEM images of Cu-NWs obtained after 30 minutes of deposition

580 **Figure 9** XRD pattern of as-prepared Cu NWs after template dissolution

581 **Figure 10** CV in the presence of 1mM of nitrate ions using Cu NWs electrode

582 **Figure 11** Effect of solution pH on the peak current relative to the detection of 3.5 ppm of nitrate
583 ions

584 **Figure 12** Effect of nanostructures length on the intensity of peak current of nitrate ions detection

585 **Figure 13** Effect of increasing nitrate ions concentration using Cu NWs electrode obtained with 60
586 min of galvanic deposition

587 **Figure 14** (a) Interference of 500 ppm of different chemical species (b) interference of chlorine on
588 the peak current for the detection of 50 ppm of nitrate ions

589 **Figure 8** Real samples analysis. (a-b) Rain water (c-d) water from Oreto river.

590 **Figure 9** LSV experiment carried out with commercial drinking water

591